OXFORD | Society of Toxicology
www.toxsci.oxfordjournals.org

Evidence for Aryl hydrocarbon Receptor-Mediated Inhibition of Osteoblast Differentiation in Human Mesenchymal Stem Cells

AtLee T. D. Watson,* Rachel C. Nordberg,[†] Elizabeth G. Loboa,[†,‡] and Seth W. Kullman*,[§,1]

*Department of Biological Sciences, North Carolina State University, Raleigh, North Carolina 27695 and [†]University of North Carolina at Chapel Hill and North Carolina State University Joint Department of Biomedical Engineering, Raleigh, North Carolina 27695 and Chapel Hill, North Carolina 27599; [‡]College of Engineering, University of Missouri, Columbia, Missouri 65211; and [§]Center for Human Health and the Environment, North Carolina State University, Raleigh, North Carolina 27695

[1]To whom correspondence should be addressed at Campus Box 7633, Raleigh, NC 27695-7633. Fax: (919) 515-7169. E-mail: swkullma@ncsu.edu.

The authors certify that all research involving human subjects was done under full compliance with all government policies and the Helsinki Declaration.

ABSTRACT

Multipotent mesenchymal stem cells (MSCs) maintain the ability to differentiate into adipogenic, chondrogenic, or osteogenic cell lineages. There is increasing concern that exposure to environmental agents such as aryl hydrocarbon receptor (AhR) ligands, may perturb the osteogenic pathways responsible for normal bone formation. The objective of the current study was to evaluate the potential of the prototypic AhR ligand 2,3,7,8-tetrachlorodibenzo-*p*-dioxin (TCDD) to disrupt osteogenic differentiation of human bone-derived MSCs (hBMSCs) *in vitro*. Primary hBMSCs from three donors were exposed to 10 nM TCDD and differentiation was interrogated using select histological, biochemical, and transcriptional markers of osteogenesis. Exposure to 10 nM TCDD resulted in an overall consistent attenuation of alkaline phosphatase (ALP) activity and matrix mineralization at terminal stages of differentiation in primary hBMSCs. At the transcriptional level, the transcriptional regulator *DLX5* and additional osteogenic markers (*ALP*, *OPN*, and *IBSP*) displayed attenuated expression; conversely, *FGF9* and *FGF18* were consistently upregulated in each donor. Expression of stem cell potency markers *SOX2*, *NANOG*, and *SALL4* decreased in the osteogenic controls, whereas expression in TCDD-treated cells resembled that of undifferentiated cells. Coexposure with the AhR antagonist GNF351 blocked TCDD-mediated attenuation of matrix mineralization, and either fully or partially rescued expression of genes associated with osteogenic regulation, extracellular matrix, and/or maintenance of multipotency. Thus, experimental evidence from this study suggests that AhR transactivation likely attenuates osteoblast differentiation in multipotent hBMSCs. This study also underscores the use of primary human MSCs to evaluate osteoinductive or osteotoxic potential of chemical and pharmacologic agents *in vitro*.

Key words: aryl hydrocarbon receptor; 2,3,7,8-tetrachlorodibenzo-*p*-dioxin; TCDD; mesenchymal stem cell; osteoblast differentiation; skeletal toxicity; bone toxicity.

Bone-related disorders represent a significant health concern among both developing and aging demographics. Skeletal dysplasias, typically diagnosed early in life, arise from mutations in genes responsible for patterning and growth of bone and cartilage structures and result in functional deficits during development (Krakow and Rimoin, 2010). Conversely, degenerative bone diseases such as osteopenia and osteoporosis involve a loss of bone mineral density and are more prevalent in elderly

individuals (Briggs et al., 2016). These outcomes may be influenced by exposure to chemical agents in the environment. For example, tobacco smoke exposure is associated with reduced bone mineral density, increased fracture risk, and increased risk of osteoporosis and rheumatoid arthritis (Klareskog et al., 2007; Ward and Klesges, 2001).

At the cellular level, osteoblasts are the key drivers of bone formation during development and later in maintaining skeletal homeostasis (Long, 2012). Osteoblasts are derived from multipotent mesenchymal stem cells (MSCs) that commit to preosteoblasts and undergo differentiation to form functionally mature osteoblasts. Osteoblast differentiation integrates a milieu of signaling mediators derived from canonical developmental pathways [WNT, FGF, bone morphogenetic protein (BMP), Notch, and Hedgehog], which converge to influence the expression and/or activity of the "master" transcriptional regulators of osteoblastogenesis, runt-related transcription factor 2 (RUNX2) and osterix (OSX, or SP7) (Jensen et al., 2010; Sinha and Zhou, 2013).

Following early differentiation events, osteoblasts secrete collagenous and noncollagenous proteins to comprise the bone extracellular matrix (ECM) which then undergoes mineralization to form ossified bone with its characteristic mechanical and structural integrity. Alkaline phosphatase (ALP) plays a critical role during these early stages of bone mineralization and is a well-recognized marker of osteogenic activity. ALP hydrolyzes extracellular pyrophosphate (ePP_i) to inorganic phosphate (P_i), which then complexes with extracellular calcium ions to form hydroxyapatite (HA) mineral, a defining hallmark of ossified bone *in vivo* and mature osteoblasts *in vitro* (Golub and Boesze-Battaglia, 2007). The composition of the bone ECM also plays an important role in osteoblast differentiation (Baroncelli et al., 2018). Although collagenous proteins such as *collagen type 1 alpha 1* (COL1A1) comprise 80%–90% of bone ECM, noncollagenous proteins also regulate osteoid mineralization by serving as nucleation sites for HA crystal formation. Among these are *osteocalcin/bone gamma-carboxyglutamate protein* (OSC/BGLAP), *secreted protein acidic and cysteine rich/osteonectin* (SPARC), *osteopontin/secreted phosphoprotein 1* (OPN/SPP1), *integrin-binding sialoprotein/bone sialoprotein 2* (IBSP/BSP2) (Komori, 2010).

Although the underlying mechanisms of osteogenesis are generally well described, significant gaps remain in our understanding of how exposure to environmental toxicants may alter the transcriptional networks governing osteoblast differentiation and bone growth. Given the multipotent nature of MSCs and their ability to differentiate into osteogenic, chondrogenic, or adipogenic lineage, certain classes of toxicants may shunt MSC differentiation to favor one lineage over another. For instance, the retinoid X receptor (RXR) agonist tributyltin and peroxisome proliferator-activated receptor gamma (PPARγ) agonist triphenyl phosphate both promote adipogenic differentiation of MSCs in lieu of osteogenesis (Pillai et al., 2014; Watt and Schlezinger, 2015). As a result, deficits in osteoblast number and/or function may perturb skeletal development exacerbate loss of bone mineral content in aging individuals.

Aryl hydrocarbon receptor (AhR) ligands are another class of chemicals suspected of altering pathways involved in skeletal development. The AhR is a basic-helix-loop-helix Per-ARNT-Sim (bHLH-PAS) transcription factor and functions as a master regulator of drug metabolism and cell signaling pathways modulating cell proliferation, differentiation and apoptosis (Abel and Haarmann-Stemmann, 2010; Chopra and Schrenk, 2011). Sources of AhR ligands in the environment include industrial processes (ATSDR, 1998), contaminated food

(Fernández-González et al., 2015), and tobacco smoke (Narkowicz et al., 2013). Benzo[a]pyrene (BaP), polychlorinated biphenyls (PCBs), and polychlorinated dibenzodioxins/dibenzofurans (PCDDs/PCDFs) have received the most attention based on their potential for exposure, affinity for the AhR, and reported toxicity to pathways involving cell proliferation, and growth and differentiation in multiple organ systems. In terms of skeletal development, the potent PCDD congener, 2,3,7,8-tetrachlorodibenzo-*p*-dioxin (TCDD) has been shown to inhibit adipogenic (Liu et al., 1996) and chondrogenic (Dong et al., 2012; Kung et al., 2012) differentiation in both *in vivo* and *in vitro* model systems. Although numerous studies have examined AhR-mediated osteotoxicity in rodent, teleost, and select osteoblast *in vitro* models (Korkalainen et al., 2009; Ryan et al., 2007; Watson et al., 2017), few studies have investigated the impact of TCDD on osteogenic differentiation of human MSCs.

In the current study, we investigate the influence of TCDD on osteoblast differentiation in human bone-derived MSCs (hBMSCs) isolated from three donors. We provide evidence that AhR transactivation with 10 nM TCDD modulates histological, biochemical, and transcriptional processes associated with multipotency, osteoblast differentiation and extracellular matrix deposition.

MATERIALS AND METHODS

hBMSC isolation and characterization. Excess human bone fragments were obtained during elective procedures at the University of North Carolina-Chapel Hill hospitals (IRB exemption protocol: 10-0201). Human MSC cells were isolated and characterized as described previously (Charoenpanich et al., 2014; Sakaguchi et al., 2004). Briefly, bone fragments were washed in phosphate-buffered saline (PBS) containing 100 U/mL penicillin and 100 mg/mL streptomycin (Corning, Inc.). The bone fragments were minced into approximately 1 mm^3 cubes using a scalpel and digested in a 3 mg/ml collagenase XI solution (Sigma-Aldrich) on an orbital shaker for 3 h at 37°C. The digest solution was filtered through a 100-μm cell strainer, centrifuged at 500 × g for 5 min to pellet the cells, and the cells were resuspended in growth medium (GM) comprised of minimal essential medium, α-modification (MEM-α, GE Healthcare) supplemented with 10% fetal bovine serum (FBS, Rocky Mountain Biologicals), 2 mM L-glutamine (Genesee Scientific), 100 U/ml penicillin, and 100 μg/ml streptomycin (Genesee Scientific). Cell suspensions were plated and incubated overnight under standard cell culture conditions of 37°C at 5% CO_2 in a humidified incubator, henceforth referred to as "standard culture conditions". After 24 h, plates were rinsed with PBS to wash out the nonadherent cells population and the media was replaced with fresh GM.

A preliminary assessment was conducted to characterize the proliferation and differentiation potential of donor hBMSCs as modified from Bernacki et al. (2008). At passage 0, hBMSCs were plated in 6-well tissue culture-treated plates (Genesee Scientific) at a density of 0.6×10^4 cells/cm^2 in GM. After 24 h, the media was changed to either GM, osteogenic differentiation medium (ODM) comprised of α-MEM supplemented with 10% FBS, 2 mM L-glutamine, 100 U/ml penicillin, and 100 μg/ml streptomycin, 50 μM ascorbic acid (Sigma-Aldrich), 0.1 μM dexamethasone (Sigma-Aldrich), and 10 mM β-glycerophosphate (Sigma-Aldrich), or adipogenic differentiation medium (ADM) comprised of α-MEM supplemented with 10% FBS, 2 mM L-glutamine, 100 U/ml penicillin and 100 μg/ml streptomycin, 1 μM dexamethasone (Sigma-Aldrich), 5 μg/ml h-insulin (Sigma-Aldrich), 100 μM indomethacin (Sigma-Aldrich), and 500 μM isobutylmethylxanthine (IBMX,

Table 1. Age, Sex, and Osteoporotic Status of hBMSC Donors 1–3 Used for Osteogenic and Adipogenic (Only Donor 1) Differentiation Experiments

Donor	Sex	Age (years)	Osteoporosis
1	Female	25	No
2	Male	64	No
3	Female	95	Yes

Sigma-Aldrich). Media was changed every 3–4 days and cells were assessed for mineralization (14–17 days) and lipid accumulation (17–24 days) as markers of terminal differentiation. Any hBMSC population with aberrant staining patterns (ie, significant lipid accumulation in ODM, or significant calcium accretion in ADM) was excluded from the study. Based on these criteria, hBMSCs from three donors (Table 1) were selected and used in subsequent experiments.

TCDD experiments. Frozen hBMSCs at passage 0 were thawed, cultured, and expanded in GM under standard culture conditions. hBMSCs between passages 3 and 6 were seeded into 6- or 12-well tissue culture treated plates (Genesee Scientific) at density of 1×10^4 cells/cm^2 in GM. After 24 h, media was replaced with ODM or ADM to induce differentiation (day 0). Osteogenic differentiation experiments were conducted with hBMSCs from Donors 1 to 3; adipogenic differentiation was assessed in Donor 1 hBMSCs only. For osteogenic experiments, cells were cultured for up to 17 days in ODM containing one of the following treatments: 0.1% dimethyl sulfoxide (DMSO, vehicle control), 0.01–10 nM 2,3,7,8-tetrachlorodibenzo-*p*-dioxin (TCDD, Cambridge Isotopes Laboratory), 100 nM GNF351 (Sigma-Aldrich), or 10 nM TCDD + 100 nM GNF351 dissolved in DMSO as a vehicle. For adipogenic differentiation experiments, Donor 1 hBMSCs cultured in ADM were treated with 0.1% DMSO or 10 nM TCDD for 24 days. Negative controls included undifferentiated cells cultured in GM containing 0.1% DMSO. For all experiments, dosed media was replaced every 3–4 days and cells were maintained under standard culture conditions for the duration of the experiment.

Cell viability. Cell viability of hBMSCs cultured in GM and ODM dosed with TCDD was assessed using a resazurin-based assay. Positive controls containing 0.1% Triton X-100 were included for both GM and ODM plates. Briefly, cells were seeded into 96-well opaque-walled tissue culture plates at a density of 1.0×10^4 cells/cm^2 in 100 µl of dosed media. At 24 and 48 h postseeding, 20 µl of 0.15 mg/ml resazurin (pH 7.4, 0.2-µm filtered) was added to each well and plates were incubated for 2 h under standard culture conditions. Fluorescence was measured using FLUOstar spectrophotometer using 560 nm/590 nm excitation/emission parameters and cell viability was reported as a percentage normalized to vehicle controls.

Mineralization assays. Cell monolayers were stained with Alizarin Red S at 14–17 days post induction (dpi) of differentiation to label mineralized extracellular matrix. Briefly, cells were washed twice in PBS, fixed in 10% neutral buffered formalin for 20 min, washed twice with ddH$_2$O, and stained for 15 min with 40 mM Alizarin Red S. Stained monolayers were washed five times in ddH$_2$O and representative wells were imaged.

Additional wells run in parallel were used to quantify calcium accretion using the colorimetric-based Calcium (CPC) LiquiColor Assay (EKF Diagnostics-Stanbio Laboratory). After washing with PBS, 250 µl of 0.5 N HCl was added, the contents of each well were harvested by scraping, and samples were shaken at 500 rpm for 24–48 h at 4°C. Samples were centrifuged at 3000 ×g for 3 min, and the supernatants were dispensed in a clear, flat-bottom 96-well plate. The colorimetric solution was added, and plates were incubated for 45 min. Absorbance was measured at 550 nm and total calcium content was derived from a standard curve using linear regression analysis. Calcium content was normalized to total protein concentration quantified using the Pierce BCA Protein Assay Kit (ThermoScientific) from samples run in parallel. For each sample, absorbance was measured at 560 nm and protein concentrations were derived from a standard curve using linear regression analysis of known concentrations of bovine serum albumin.

Inorganic phosphate was measured from the media at 17 dpi using the QuantiChrom Phosphate Assay Kit (BioAssay Systems, Hayward, California) according to the manufacturer's instructions. Briefly, media aliquots were diluted in ddH$_2$O, combined with reagent in a 96-well plate, and incubated at room temperature for 30 min. Absorbance was measured at 620 nm for all samples and phosphate concentration was derived from a standard curve of known concentrations using linear regression analysis.

Adipogenic assays measuring lipid accumulation. Cells were stained with Oil Red O and subsequently destained to assess adipogenesis in hBMSCs cultured in ODM and ADM. Cells were washed with PBS, fixed in 10% neutral buffered formalin for 30 min, and washed twice with ddH$_2$O. Wells were washed with 60% isopropyl alcohol and then stained for 5 min in filtered Oil Red O staining solution composed of three parts 30 mg/ml Oil Red O in 100% isopropyl alcohol to two parts ddH$_2$O. Wells were washed with ddH$_2$O and imaged under light microscopy. To quantify lipid accumulation, wells were aspirated, allowed to dry, and destained via addition of 60% isopropyl alcohol. Absorbance of destain solution was measured at 500 nm and Oil Red O concentrations were determined from a standard curve measuring known Oil Red O standards.

ALP assays. Immunohistochemical staining for ALP was measured at 7 dpi using Blue Color AP Staining Kit (Systems Biosciences). Cells were washed in PBS, fixed in 10% neutral buffered formalin, and incubated in substrate solution for 30 min. Next, cells were washed twice in PBS and imaged under light microscopy (Nikon SMZ1500) at 10× magnification. Alkaline phosphatase activity was measured using the Sensolyte pNPP Alkaline Phosphatase Assay Kit (Anaspec). Briefly, cells were rinsed in assay buffer, scraped, and incubated under agitation for 10 min at 4°C. Samples were centrifuged at 3000×g for 10 min and supernatants were collected. In a 96-well plate format, 30 µl of *p*-Nitrophenyl phosphate was added to each sample or standard in triplicate and incubated for 30 min at 37°C. Absorbance was measured at 405 nm and ALP activity was derived from a standard curve using linear regression analysis from known ALP concentrations. For each sample, ALP activity was normalized to total protein concentration quantified as described above.

qPCR. hBMSCs were lysed in TRI Reagent (Ambion, Life Technologies) and total RNA was isolated according to the manufacturer's instructions. Total RNA was quantified using Agilent 2100 Bioanalyzer and 2100 Expert Software package (Agilent Technologies). RNAs with RNA Integrity numbers (RINs) lower than 9 were excluded. Next, cDNA was synthesized from 1 µg of total RNA using High Capacity cDNA Reverse Transcription Kit
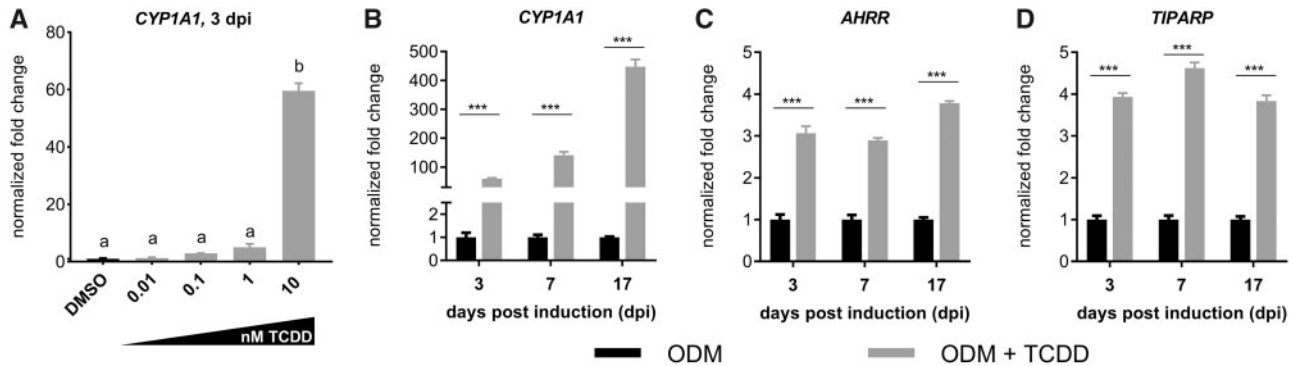
Figure 1. qPCR assessment of AhR-responsive gene targets in Donor 1 hBMSCs following exposure to vehicle (DMSO) or 10 nM TCDD in ODM. (A), *CYP1A1* expression increases in concentration-dependent manner at 3 dpi. A time-course response is shown for (B) *CYP1A1*, (C) *AHRR*, and (D) *TIPARP* expression on 3, 7, and 17 dpi. Gene expression data represent mean±SEM ($n = 3$–4 technical replicates) fold change normalized to *RPL13A* expression. Groups with different letters above bars in (A) are statistically different from each another (one-way ANOVA, Tukey's post hoc test, $p < .05$); asterisks in (B)–(D) indicate statistical significance between DMSO and 10 nM TCDD groups at each timepoint (Student's two-tailed *t*-test; $^*p < .05$; $^{**}p < .01$; $^{***}p < .001$).

(Applied Biosystems) containing random primers, MultiScribe Reverse Transcriptase, RNase inhibitor, deoxynucleotide triphosphate mix, and 10× reverse transcription buffer in a 20 µl reaction. Human-specific real-time PCR primer sequences were designed in Primer3 or obtained from PrimerBank (Spandidos *et al.*, 2010) (Supplementary Table 1) and procured from IDT (Integrated DNA Technologies). Primers sets were first tested to ensure efficient amplification of the target exon sequence. To quantify relative gene expression, cDNA from control and treated samples were PCR amplified in triplicate in 96-well PCR plates (Olympus Plastics, Genesee, San Diego, California) using an Applied Biosystems 7300 Real Time PCR System. Each 15 µl-reaction was comprised of 7.5 µl of SYBR Green Real-Time PCR Master Mix (Life Technologies), 5.1 µl UltraPure Distilled H_2O (Life Technologies), 0.6 µl of 10 µM forward primer, 0.6 µl of 10 µM reverse primer, and 1.2 µl of cDNA. The conditions for each reaction were as follows: (1) 50°C for 2 min, (2) 95°C for 10 min, (3) 95°C for 15 s followed by 60°C for 60 s, repeated 40×, and (4) 95°C for 15 s, 60°C for 60 s, 95°C for 15 s, and 60°C for 15 s to derive dissociation or melt curves and ensure specificity for each primer set used. Threshold cycle (C_t) values for each reaction were determined by the ABI 7300 software package and each gene was normalized to *RPL13A*, and relative gene expression was calculated according to the $\Delta\Delta C_t$ method.

Statistical analysis. Unless otherwise noted, data from Donor 1 are presented in the text as the representative hBMSC line, and additional data from Donors 2 and 3 can be found in the Supplementary Data. Data are presented as the mean ±SEM ($n = 3$–4 technical replicates per donor). Pairwise comparisons between ODM-DMSO versus ODM-TCDD were conducted using an unpaired, two-tailed Student's *t*-test. Comparisons between two or more conditions were analyzed using a one-way analysis of variance (ANOVA) with a Tukey's post hoc test to for multiple comparisons. For all statistical analyses, the threshold for significance was set to $\alpha = 0.05$ with p-values $<.05$ deemed significant.

RESULTS

hBMSCs are Responsive to AhR Transactivation Following TCDD Treatment

Cytotoxicity was assessed in TCDD-exposed hBMSCs from Donor 1 cultured in GM and ODM. At 24 and 48 h post seeding,

cell viability was not impacted following exposure to 1 and 10 nM TCDD (Supplementary Figure 1). Next, hBMSCs were examined to assess their responsiveness to AhR transactivation through quantitative assessment of select AhR gene markers. At 3 dpi, TCDD significantly induced *CYP1A1* expression in a concentration-dependent manner (Figure 1A) and induction was maintained for the duration of the experiment (Figure 1B). Other AhR-responsive genes including *AHRR* and *TIPARP* displayed elevated expression throughout the experiment when compared with cells under ODM conditions (Figs. 1C and 1D; Supplementary Table 2). Based on these data, hBMSCs were treated with 10 nM TCDD for subsequent experiments to investigate the potential for AhR-mediated inhibition of hBMSC differentiation.

hBMSCs Differentiate Into Osteoblasts Under Osteogenic Conditions

hBMSCs from three donors (Table 1) were assessed to determine their osteogenic potential in the presence of GM, ODM, and ODM + TCDD. After 17 days hBMSCs cultured in GM were negative for Alizarin red staining, whereas hBMSCs cultured in ODM demonstrated robust staining of calcium-rich HA mineral. TCDD-treated cells displayed a consistent attenuation of Alizarin red staining in each donor when compared with ODM vehicle controls (Figure 2A). As components of HA mineral, calcium and inorganic phosphate (P_i) were measured from Donor 1. In both assays, cells cultured in ODM displayed a significant induction relative to GM, whereas TCDD-exposed cells despite an increase relative to GM, experienced a significant 50% reduction relative to ODM in both biochemical assays (Figs. 2B and 2C).

Based on its role in early mineralization, ALP was assayed at the transcript, enzymatic, and histochemical levels at 7 dpi. Relative to undifferentiated hBMSCs cultured in GM, hBMSCs from Donor 1 under ODM conditions demonstrated increased ALP immunohistochemical staining with a corresponding 3.2- and 3.4-fold induction in *ALP* expression and ALP enzymatic activity, respectively. By comparison, treatment with 10 nM TCDD, attenuated ALP staining and resulted in an overall 43% and 30% reduction in *ALP* expression and ALP activity respectively compared with hBMSCs cultured in ODM (Figure 3). These trends were consistent across Donors 1–3 whereby ALP activity and expression was significantly reduced in TCDD-treated hBMSCs relative to the ODM vehicle controls (Supplementary Figure 2).
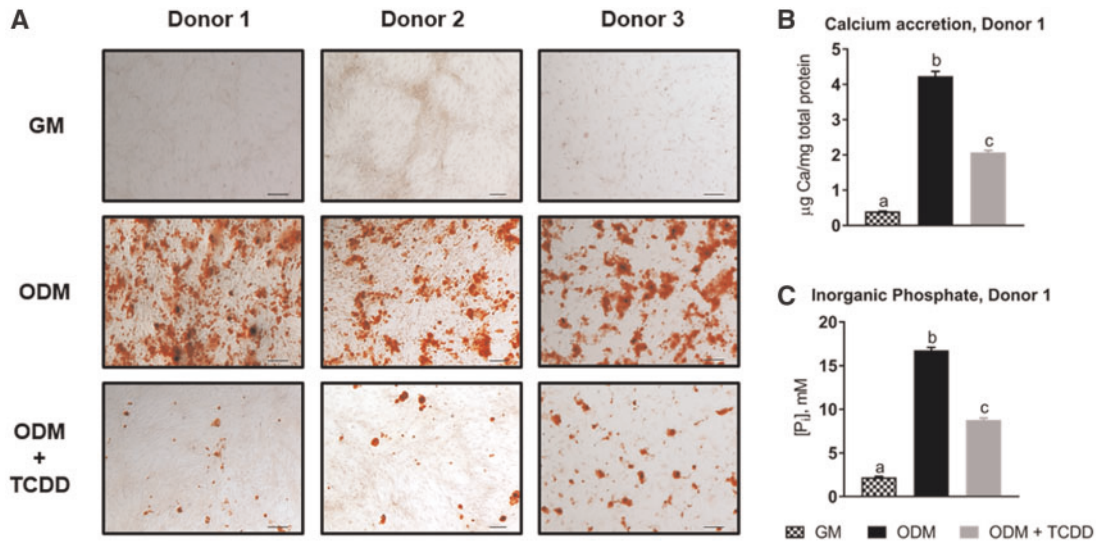
Figure 2. Apical assessment of hBMSCs from Donors 1 to 3 treated with GM, ODM, and ODM + 10 nM TCDD. A, Alizarin Red S staining was conducted at 17 dpi to evaluate mineralization potential *in vitro* (scale bar = 200 µm). B, Calcium accretion and C inorganic phosphate (Pi) were measured as constituents of HA mineral. Calcium accretion was normalized to total protein, and inorganic phosphate concentration was determined from media. Data in (B) and (C) represent mean±SEM (n = 3–4 technical replicates); groups with different letters above bars are statistically different from each another (one-way ANOVA, Tukey's post hoc test, $p < .05$).
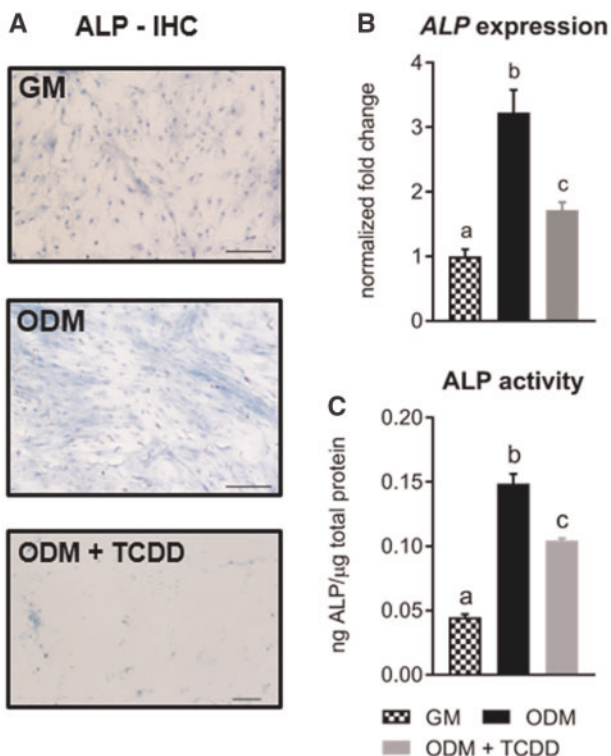

Figure 3. Alkaline phosphatase (ALP) assessment in Donor 1 hBMSCs treated with GM, osteogenic differentiation media (ODM), or ODM + 10 nM TCDD. A, Immunohistochemical staining for ALP; B, *ALP* expression; C, ALP enzymatic activity were conducted at 7 dpi. Data in (B) and (C) represent mean±SEM (n = 4 technical replicates); groups with different letters are statistically different from each another (one-way ANOVA, Tukey's post hoc test, $p < .05$). Scale bars in (A) represent 200 µm.

TCDD Attenuates Expression of Select Osteoblast-Specific Genes

Differential expression of a suite of osteogenic genes was next determined to assess the impact of TCDD treatment on hBMSC differentiation. A complete summary of osteogenic gene expression data from all donors at 3, 7, and 17 dpi can be found in Supplementary Figure 3 and Supplementary Tables 3 and 4. By 3 dpi, *DLX5* and *RUNX2* demonstrated a 2-fold or greater induction in ODM controls when compared with hBMSCs cultured under nondifferentiating GM conditions (Supplementary Figure 3). When comparing ODM versus ODM + TCDD conditions, expression of *DLX5* revealed the most consistent response across donors and across early and intermediate stages of differentiation (Figure 4A; Supplementary Table 3). Additional upstream and downstream regulators within the osteogenic regulatory pathway were also assessed and revealed similar expression profiles across donors. *TWIST1* expression was diminished in all donors at both 3 and 7 dpi except for Donor 3 at 7 dpi (Figure 4A; Supplementary Table 3). *RUNX2*, the master regulator of osteogenesis, was upregulated 1.4- to 2.1-fold at 7 dpi in all three donors, despite significant and consistent attenuation of *DLX5*, an upstream regulator of RUNX2 (Figure 4A; Supplementary Table 3). *OSX* was significantly attenuated in Donor 1 at both 3 and 7 dpi (Figure 4A). Donor 2 demonstrated a significant reduction of *OSX* at 3 dpi and slight, but not significant reduction at 7 dpi; however, *OSX* expression in Donor 3 hBMSCs appeared less responsive to TCDD treatment (Supplementary Table 3). Based on the role of FGF signaling in MSC differentiation (Su et al., 2008), expression of FGF ligands *FGF2/9/18* was also assessed at 3 and 7 dpi. TCDD exposure significantly induced expression of *FGF9* and *FGF18* at 3 and 7 dpi in all three donors with Donor 1 displaying the highest induction (Figure 4B). *FGF2* was only significantly induced in TCDD-treated cells at 3 dpi in Donor 2 (Supplementary Table 3) and Donor 1 at 7 dpi (Figure 4B).

To assess intermediate and apical stages of differentiation, expression of ECM genes (*COL1A1, OSC, OPN, OGN, IBSP, SPARC*) was measured at 7 and 17 dpi based on their respective role in matrix mineralization. Across all donors, TCDD treatment resulted in a 2-fold or greater reduction in *OPN* at both 7 and 17 dpi; conversely, *SPARC* was elevated 1.5- to 3.0-fold (Figure 4C). Other genes revealed less consistent responses across both timepoints and donors assessed. In Donor 1, *COL1A1* expression was not altered at 7 dpi in TCDD-treated
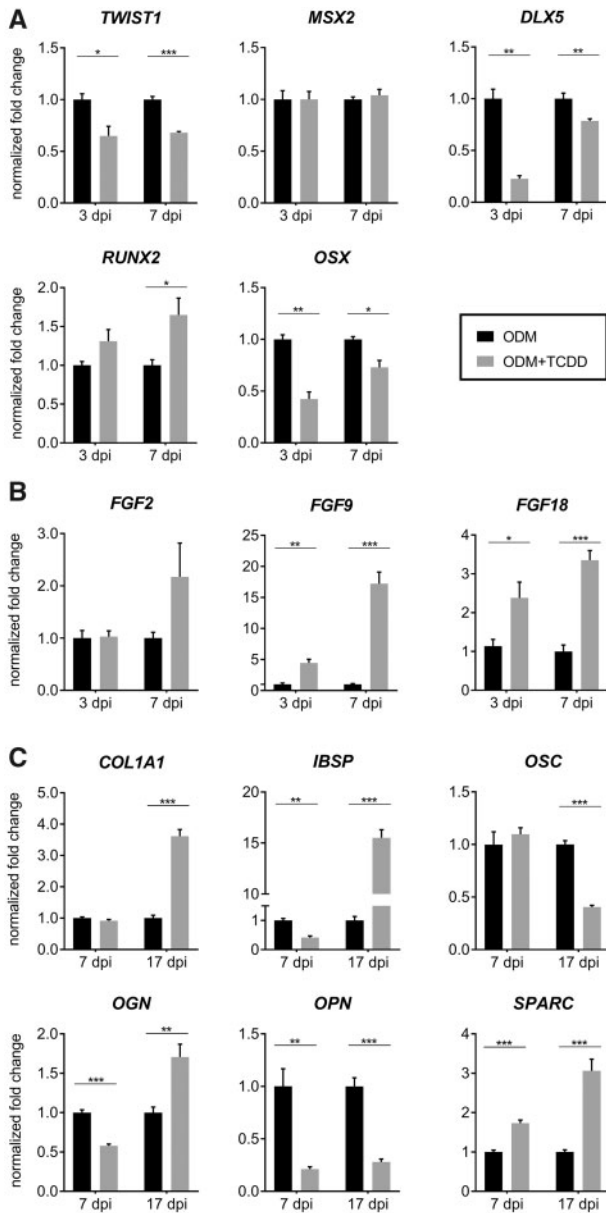
Figure 4. qPCR assessment of Donor 1 hBMSCs cultured in ODM and treated with DMSO (vehicle control) or 10 nM TCDD. Stage-specific osteogenic markers were measured for (A) transcriptional regulators at 3 and 7 dpi, (B) fibroblast growth factors (FGF) at 3 and 7 dpi, and (C) ECM markers at 7 and 17. Gene expression data represent mean±SEM fold change normalized to *RPL13A* expression (*n* = 3–4 technical replicates); asterisks denote statistical significance between DMSO and 10 nM TCDD groups at each timepoint (Student's two-tailed *t*-test; *p < .05; **p < .01; ***p < .001).

hBMSCs; however, by 17 dpi expression displayed a significant increase in expression when apical assays were conducted (Figure 4C). *IBSP* and *OGN* expression displayed a biphasic response with diminished expression at 7 dpi but elevated expression when measured at 17 dpi (Figure 4C).

AhR Inhibition Blocks TCDD-Mediated Inhibition of Osteogenesis

To confirm that observed effects are AhR-mediated, separate experiments in Donor 1 hBMSCs were repeated with 10 nM TCDD and/or 100 nM GNF351, an AhR antagonist capable of inhibiting dioxin response element (DRE)-dependent and

independent events (Smith *et al.*, 2011). Assessments of mineral deposition demonstrated that TCDD-treated hBMSCs displayed an attenuation in Alizarin red staining. Conversely, hBMSCs treated with either GNF351 alone or GNF351 + TCDD demonstrated positive Alizarin red staining that more closely resembled that of ODM controls (Figure 5A). Similarly, calcium content was partially rescued in hBMSCs coexposed to GNF351 + TCDD (Figure 5B). The impact of GNF351 exposures and GNF351 + TCDD coexposures on gene expression at 3, 7, and 14 dpi was also determined. *CYP1A1* was used as a marker of a classical AhR/DRE-mediated response and demonstrated significant induction in cells treated with TCDD alone. Comparatively, addition of 100 nM GFN351 significantly attenuated TCDD-mediated CYP1A1 induction indicating its ability to inhibit AhR signaling in hBMSCs (Figure 5C). The effect of GNF351 on expression of TCDD responsive osteogenic regulators *DLX5* (3 dpi), *FGF9* (3 dpi) and *OPN* (14 dpi), was subsequently assessed. Similar to *CYP1A* expression and calcium deposition, coexposure to GNF351 + TCDD either fully or partially rescued *DLX5*, *FGF9*, and *OPN* to levels more similar to ODM vehicle controls (Figs. 5D, 5E, and 5F). Taken together, these data suggest that *DLX5*, *FGF9*, and *OPN* are AhR responsive and may play critical roles in the ability of AhR to modulate osteogenesis *in vitro*.

TCDD Dysregulates Adipogenic Differentiation

Based on our data demonstrating the ability of TCDD to inhibit osteogenesis, the following experiments were conducted to determine whether TCDD-exposed hBMSCs favored adipogenic differentiation in lieu of osteogenic differentiation. hBMSCs from Donor 1 were exposed to TCDD in ODM and adipogenic differentiation media (ADM) and were stained with Oil Red O to assess lipid formation. By 24 dpi neither the DMSO- nor TCDD-exposed hBMSCs stained positive for Oil Red O (eg, lipid formation) under osteogenic conditions. hBMSCs cultured under adipogenic conditions stained positive for Oil Red O; however, ADM + TCDD-treated cells displayed an attenuation in Oil Red O staining relative to ADM + DMSO-treated hBMSCs (Figs. 6A and 6B). Additionally, relative mRNA expression of adipogenic markers was measured for all treatments. hBMSCs cultured in ADM displayed significantly higher expression of adipogenic markers relative to hBMSCs cultured in either GM or ODM. *PPARγ*, a nuclear receptor responsible for promoting adipogenic differentiation (Kawai *et al.*, 2010) was upregulated 6000-fold in ADM relative to GM. Another adipogenic regulator, *C/EBPα*, as well as markers of differentiated adipocytes *PLIN1* and *FABP4* were also significantly induced under ADM conditions relative to undifferentiated cells in GM. At 24 dpi hBMSCs cultured in ADM and treated with 10 nM TCDD exhibited no change in expression of *FABP4* and *C/EBPα* relative to ADM controls, however, both *PPARγ* and *PLIN1* demonstrated elevated expression that is inconsistent with the observed attenuation in overall lipid formation (Figure 6C).

TCDD Treatment Causes hBMSCs to Retain Expression of Stemness-Related Genes

Based on previous experiments demonstrating inhibition of adipogenic and osteogenic markers, we next sought to determine whether TCDD-treated hBMSCs retained expression of markers associated with undifferentiated MSCs at 17 dpi. Under osteogenic culture conditions, hBMSCs from Donor 1 demonstrate a 12-fold reduction in expression of previously validated MSC stemness markers (Riekstina *et al.*, 2009) NANOG, SOX2, and SALL4 when compared with undifferentiated hBMSCs in GM. Expression of the same genes under ODM + TCDD conditions,
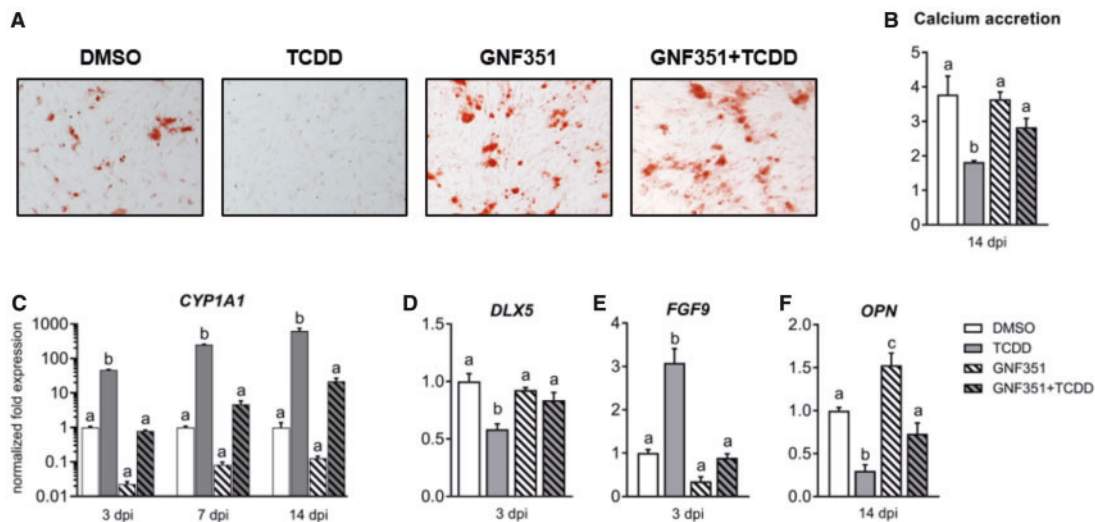
Figure 5. Osteogenic assessment of hBMSCs (Donors 1 and 2) cultured in ODM and treated with vehicle, 10 nM TCDD, and/or 100 nM GNF351. (A) Representative image of Alizarin Red S staining and corresponding calcium accretion in (B) at 14 dpi. GNF351 blocks AhR transactivation evidenced by inhibition of CYP1A1 expression at 3, 7, and 14 dpi in (C), and partial/full rescue of osteogenic markers (D) *DLX5*, (E) *FGF9*, and (F) *SPP1*. Donor 2 is shown in (A, B) and Donor 1 shown in (C-F). Data represent mean±SEM ($n = 3$–4 technical replicates) (B-F); groups with different letters are statistically different from each another (one-way ANOVA, Tukey's post hoc test, $p < .05$). Scale bars in (A) represent 200 μm.

however, remained elevated (significantly higher than ODM, $p < .05$) and more closely resembled undifferentiated hBMSCs cultured in GM. Similar expression patterns were observed with OCT4 expression, however, this data did not reach statistical significance (Figure 7). These results were consistent across Donors 1–3 (Supplementary Table 5). Expression of MSC stemness markers were then assessed following coexposures 100 nM GNF351 ± 10 nM TCDD (Donor 1 only). Similar to our results with transcriptional regulators and ECM markers, coexposure with GNF351 partially attenuated TCDD-mediated induction of *SOX2*, *NANOG*, and *SALL4* more consistent with cells incubated in ODM alone (Figure 7). Overall, these data suggest a putative linkage between AhR transactivation, multipotency regulators and osteogenic potential of hBMSCs.

DISCUSSION

An emerging theme in MSC biology suggests that extrinsic factors, including exposure to exogenous environmental agents, may perturb the regulatory networks that coordinate the balance of MSC self-renewal and/or the commitment and differentiation toward a adipogenic, chondrogenic, or osteogenic fate. In the present study, we demonstrate that exposure of primary hBMSCs to 10 nM TCDD results in the attenuation of osteogenic differentiation in hBMSCs isolated from multiple human donors. Following the addition of osteogenic differentiation media (ODM), hBMSCs were assessed for transcriptional, biochemical, and histological hallmarks of osteogenesis at early (3 dpi), intermediate (7 dpi), and apical (17 dpi) stages of differentiation. TCDD exposure significantly altered the transcriptional profile of select osteogenic regulators and ECM markers, ALP activity, and the formation of HA mineral in hBMSCs. Assessments of lipid formation and expression of adipogenic transcriptional regulators indicate that AhR activation does not promote adipogenesis over osteogenic differentiation under the conditions of this study. These data suggest that TCDD-mediated AhR transactivation likely plays an inhibitory role in osteogenic differentiation of multipotent MSCs.

TCDD and other AhR ligands have previously been shown to target differentiation of multiple cell types including hematopoietic stem cells (Singh et al., 2009), cardiomyocytes (Wang et al., 2010), chondrocytes (Dong et al., 2012; Kung et al., 2012), and adipocytes (Liu et al., 1996; Shimba et al., 2001). Our findings of reduced ALP activity and attenuated mineralization confirm similar results from other studies in preosteoblasts *in vitro* (Korkalainen et al., 2009; Ryan et al., 2007). Moreover, our findings align with those observed in a recent study by Kakutani et al. (2018) who demonstrated TCDD-mediated inhibition of both osteogenesis and adipogenesis in one hBMSC cell line.

Consistent with *in vitro* findings, exposure to TCDD and other AhR ligands is associated with altered bone formation *in vivo*. In humans, gestational exposure to PCBs is associated with reduced mineralization of teeth (Alaluusua et al., 1996), a process regulated by cementoblasts derived from dental pulp MSCs. Similar tooth enamel defects were observed in children exposed to TCDD following the Seveso, Italy incident (Alaluusua et al., 2004); however, exposure to adult females was not associated with altered bone health. TCDD exposure in adult rodent models results in altered bone size, geometry, and biomechanical strength (Herlin et al., 2010; Jämsä et al., 2001), whereas developmental TCDD exposure results in delayed ossification and attenuated bone mineral density (Finnilä et al., 2010; Miettinen et al., 2005). Conversely, C57BL/6 mice exposed to TCDD during juvenile development displayed an increase in trabecular bone volume, decreased bone marrow adiposity, and a concomitant increase in osteoblast and decrease in osteoclast numbers (Fader et al., 2018). These *in vivo* studies highlight the potential influence of timing of exposure, and the complex role that AhR transactivation plays in bone homeostasis through modulation of both osteoblast (anabolic) and osteoclast (catabolic) functions (Korkalainen et al., 2009; Yu et al., 2014).

Although the precise role of the AhR in normal bone development remains poorly understood, our data suggest that AhR may play a repressive role in osteogenesis through dysregulation of extracellular matrix deposition, early osteogenic transcriptional modifiers, and regulators of pluripotency. Apical stages of osteogenic differentiation appear to be particularly
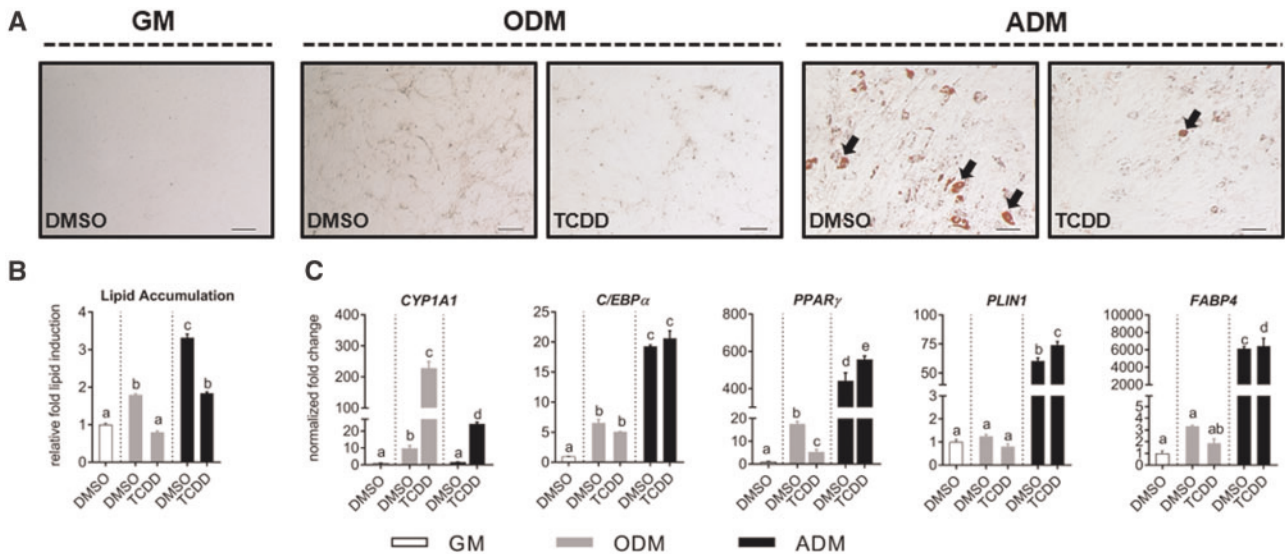
Figure 6. Adipogenic assessment of DMSO- and TCDD-treated hBMSCs in ODM and ADM at 24 dpi from Donor 1. A, Representative images of Oil Red O staining; black arrows signify positive staining of lipid vacuoles (scale bars = 200 μm). B, Lipid accumulation quantified from wells in (A). C, qPCR assessment of adipogenic markers PPARγ, C/EBPα, PLIN1, and FABP4 at 24 dpi. Data in (B) and (C) represent mean±SEM (n = 3–4 technical replicates); groups with different letters are statistically different from each another (one-way ANOVA, Tukey's post hoc test, $p < .05$).

susceptible to TCDD exposure based on our findings of attenuated mineralization and altered ECM gene expression. Although bone ECM composition is a critical determinant of bone structural integrity, it can also serve as scaffold or template to promote osteogenic differentiation in vitro. BMSCs cultured on devitalized ECM from differentiated osteoblasts displayed a marked increase in osteogenic differentiation relative to BMSCs cultured on ECM from undifferentiated cells (Baroncelli et al., 2018). In this study, DLX5, an early osteogenic regulator whose expression in vitro is associated with osteogenic potential of BMSCs was significantly attenuated in TCDD-treated hBMSCs from all donors at early and intermediate stages of differentiation. Conversely, FGF9 and FGF18 induction was observed in all three hBMSC donors. The observed induction of FGF9 in this study is consistent with studies in lung adenocarcinoma cells demonstrating FGF9 induction following exposure to TCDD, benzo[a]pyrene, and other AhR ligands (Ueng et al., 2005; Wang et al., 2009). Both FGF9 and FGF18 are important in bone and cartilage development; however, their respective roles in MSC commitment and differentiation may depend on cell type and developmental stage (Fakhry et al., 2005). FGF9 is associated with inhibition of osteogenic differentiation in human dental pulp MSCs and rat BMSCs (Lu et al., 2015) and calvaria-derived MSCs (Lu et al., 2014). On the other hand, FGF18 treatment in rat BMSCS appears to promote osteogenesis in vitro (Jeon et al., 2012). Moreover, FGF-FGFR signaling regulates SOX2 (Mansukhani et al., 2005). SOX2 has been shown to inhibit osteogenic differentiation of human MSCs in vitro (Ding et al., 2012; Mansukhani et al., 2005; Seo et al., 2011), suggesting a possible link between TCDD-mediated induction of FGF9/18 observed in this study and the control of MSC multipotency.

Therefore, we next investigated whether markers of pluri-/multipotency (SOX2, OCT4, NANOG, and SALL4) were affected by TCDD exposure. The proteins encoded by these genes control potency of embryonic stem (ES) cells (Wang et al., 2012), and also modulate the proliferative capacity and self-renewal of multipotent MSCs (Greco et al., 2007; Riekstina et al., 2009). Here,

we observed attenuated expression of SOX2, NANOG, and SALL4 when hBMSCs were transitioned from standard growth media (GM) to osteogenic conditions in conjunction with robust mineralization and differentiation of hBMSCs toward mature osteoblasts. By comparison, TCDD treatment abrogated attenuation of SOX2, NANOG, and SALL4 consistent with the loss of osteogenic differentiation in ODM. The expression profile of these pluri-/multipotency markers in TCDD-treated hBMSCs was more consistent with undifferentiated cells cultured in GM. Interestingly, hBMSCs cotreated with GNF351 and TCDD appeared to rescue the attenuation of NANOG and SOX2, suggesting that TCDD-mediated AhR transactivation may directly modulate osteogenic differentiation through dysregulation of pluri-/multipotency factors.

Recent studies have investigated the function of the AhR in maintaining pluripotency in vitro. AhR antagonism has previously been shown to regulate the stem cell pool of hematopoietic stem cells, suggesting that the AhR modulates proliferation and self-renewal of stem cells (Boitano et al., 2010). In ES cells, there is evidence that AhR and multipotency factors exhibit reciprocal regulation. AhR expression is directly repressed by the binding of OCT4/SOX2/NANOG protein complexes on the distal enhancer of the AhR promoter (Ko et al., 2014) and AhR derepression appears to downregulate OCT4 and SOX2 (Ko et al., 2016). This association may represent a direct regulatory loop that enables AhR to modulate pluripotent and/or differentiation in ES cells. Conversely, our findings in multipotent hBMSCs demonstrate elevated expression of pluri-/multipotency markers SOX2, NANOG, and OCT4 in response to TCDD exposure. Moreover, AhR antagonism via GNF351 results in an overall lower basal expression of these markers compared with undifferentiated cells. The relationship between AhR activation and expression of pluri-/multipotency markers in hBMSCs in this study may reflect functional differences between pluripotent stem cells and multipotent hBMSCs that are further along the differentiation continuum. Further work is needed to determine whether AhR transactivation directly or indirectly dysregulates expression of pluri-/multipotency markers, or alternatively, if
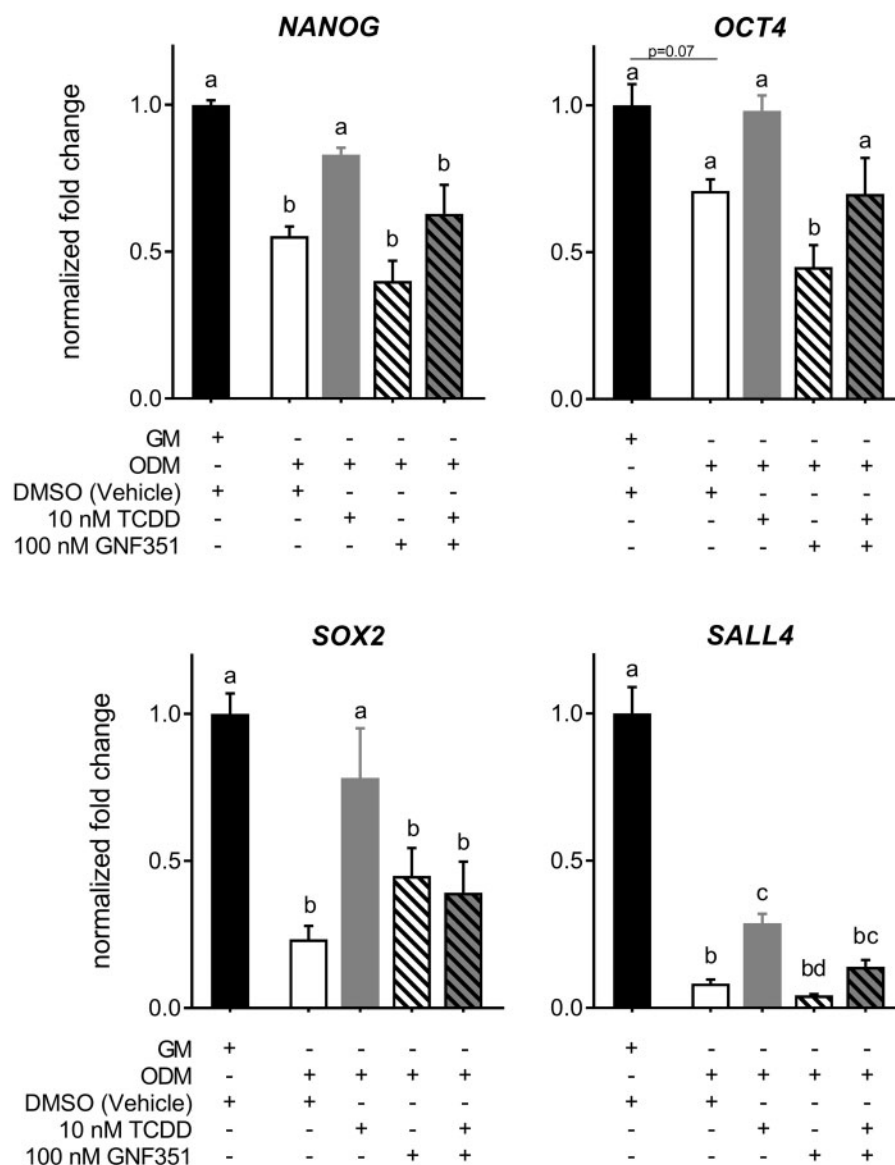
Figure 7. qPCR assessment of MSC stemness markers SOX2, OCT4, NANOG, and SALL4 at 17 dpi for Donor 1 hBMSCs cultured in GM, osteogenic differentiation media (ODM), or ODM + 10 nM TCDD. Data represent mean±SEM ($n = 3$–4 technical replicates); groups with different letters are statistically different from each other (one-way ANOVA, Tukey's post hoc test, $p < .05$).

these observed patterns simply reflect a less differentiated state in hBMSCs.

Lastly, we investigated if AhR activation shunts MSC programming to promote adipogenesis over osteogenic commitment and differentiation. Results from this analysis suggest that AhR activation does not enhance the adipogenesis in lieu of osteogenesis. Our data are consistent with previous studies that demonstrate an inhibitory effect of AhR on adipogenesis in human MSCs (Kakutani et al., 2018; Podechard et al., 2009) and in the 3T3-L1 preadipocyte model (Shimba et al., 2001). Although we demonstrate that expression of select adipogenic markers remained unchanged with addition of TCDD under ADM conditions, expression of PPARγ was increased. It is plausible that other adipogenic regulators not included in this assessment are sensitive to AhR transactivation, or alternatively, AhR transactivation plays a more prevalent role during lineage commitment of hBMSCs.

Overall, the dysregulation of MSCs during early development may provide additional support for Developmental Origins of Health and Disease hypothesis (Barker, 2007). In humans, peak bone mineral content attained during childhood and adolescence is one significant factor that determines loss of bone mineral density and fracture risk later life (McCormack et al., 2017), emphasizing the critical role of early bone formation in determining skeletal health into adulthood. Thus, through early modulation of MSC differentiation into bone-forming osteoblasts, AhR signaling may play a mechanistic role in the pathogenesis of certain developmental and/ or degenerative bone diseases. Overall, this study provides a broader understanding of putative mechanisms driving chemically induced adverse outcomes in MSCs and provides new insight into novel links between AhR-mediated gene regulation and MSC multipotency which may help inform human health risk.

SUPPLEMENTARY DATA

Supplementary data are available at *Toxicological Sciences* online.

ACKNOWLEDGMENTS

FUNDING

REFERENCES

Abel, J., and Haarmann-Stemmann, T. (2010). An introduction to the molecular basics of aryl hydrocarbon receptor biology. *Biol. Chem.* **391**, 1235–1248.

Alaluusua, S., Calderara, P., Gerthoux, P. M., Lukinmaa, P.-L., Kovero, O., Needham, L., Patterson, D. G., Tuomisto, J., and Mocarelli, P. (2004). Developmental dental aberrations after the dioxin accident in Seveso. *Environ. Health Perspect.* **112**, 1313–1318.

Alaluusua, S., Lukinmaa, P.-L., Vartiainen, T., Partanen, M., Torppa, J., and Tuomisto, J. (1996). Polychlorinated dibenzo-p-dioxins and dibenzofurans via mother's milk may cause developmental defects in the child's teeth. *Environ. Toxicol. Pharmacol.* **1**, 193–197.

ATSDR. (1998). Toxicological profile for chlorinated dibenzo-p-dioxins. Atlanta, GA: Agency for Toxic Substances and Disease Registry, U.S. Department of Health and Human Services, Public Health Service.

Barker, D. J. P. (2007). The origins of the developmental origins theory. *J. Intern. Med.* **261**, 412–417.

Baroncelli, M., van der Eerden, B. C., Kan, Y.-Y., Alves, R. D., Demmers, J. A., van de Peppel, J., and van Leeuwen, J. P. (2018). Comparative proteomic profiling of human osteoblast-derived extracellular matrices identifies proteins involved in mesenchymal stromal cell osteogenic differentiation and mineralization. *J. Cell Physiol.* **233**, 387–395.

Bernacki, S. H., Wall, M. E., and Loboa, E. G. (2008). Isolation of human mesenchymal stem cells from bone and adipose tissue. *Methods Cell Biol.* **86**, 257–278.

Boitano, A. E., Wang, J., Romeo, R., Bouchez, L. C., Parker, A. E., Sutton, S. E., Walker, J. R., Flaveny, C. A., Perdew, G. H., Denison, M. S., *et al.* (2010). Aryl hydrocarbon receptor antagonists promote the expansion of human hematopoietic stem cells. *Science* **329**, 1345–1348.

Briggs, A. M., Cross, M. J., Hoy, D. G., Sànchez-Riera, L., Blyth, F. M., Woolf, A. D., and March, L. (2016). Musculoskeletal health conditions represent a global threat to healthy aging: a report for the 2015 World Health Organization World Report on Ageing and Health. *Gerontologist* **56**, S243–S255.

Charoenpanich, A., Wall, M. E., Tucker, C. J., Andrews, D. M. K., Lalush, D. S., Dirschl, D. R., and Loboa, E. G. (2014). Cyclic tensile strain enhances osteogenesis and angiogenesis in mesenchymal stem cells from osteoporotic donors. *Tissue Eng. A* **20**, 67–78.

Chopra, M., and Schrenk, D. (2011). Dioxin toxicity, aryl hydrocarbon receptor signaling, and apoptosis-persistent pollutants affect programmed cell death. *Crit. Rev. Toxicol.* **41**, 292–320.

Ding, D., Xu, H., Liang, Q., Xu, L., Zhao, Y., and Wang, Y. (2012). Over-expression of Sox2 in C3H10T1/2 cells inhibits osteoblast differentiation through Wnt and MAPK signalling pathways. *Int. Orthop.* **36**, 1087–1094.

Dong, W., Hinton, D. E., and Kullman, S. W. (2012). TCDD disrupts hypural skeletogenesis during medaka embryonic development. *Toxicol. Sci.* **125**, 91–104.

Fader, K. A., Nault, R., Raehtz, S., McCabe, L. R., and Zacharewski, T. R. (2018). 2,3,7,8-Tetrachlorodibenzo-p-dioxin dose-dependently increases bone mass and decreases marrow adiposity in juvenile mice. *Toxicol. Appl. Pharmacol.* **348**, 85–98.

Fakhry, A., Ratisoontorn, C., Vedhachalam, C., Salhab, I., Koyama, E., Leboy, P., Pacifici, M., Kirschner, R. E., and Nah, H.-D. (2005). Effects of FGF-2/-9 in calvarial bone cell cultures: differentiation stage-dependent mitogenic effect, inverse regulation of BMP-2 and noggin, and enhancement of osteogenic potential. *Bone* **36**, 254–266.

Fernández-González, R., Yebra-Pimentel, I., Martínez- Carballo, E., and Simal-Gándara, J. (2015). A critical review about human exposure to polychlorinated dibenzo-p-dioxins (PCDDs), polychlorinated dibenzofurans (PCDFs) and polychlorinated biphenyls (PCBs) through Foods. *Crit. Rev. Food Sci. Nutr.* **55**, 1590–1617.

Finnilä, M. A. J., Zioupos, P., Herlin, M., Miettinen, H. M., Simanainen, U., Håkansson, H., Tuukkanen, J., Viluksela, M., and Jämsä, T. (2010). Effects of 2,3,7,8-tetrachlorodibenzo-p-dioxin exposure on bone material properties. *J. Biomech.* **43**, 1097–1103.

Golub, E. E., and Boesze-Battaglia, K. (2007). The role of alkaline phosphatase in mineralization. *Curr. Opin. Orthop.* **18**, 444–448.

Greco, S. J., Liu, K., and Rameshwar, P. (2007). Functional similarities among genes regulated by Oct4 in human mesenchymal and embryonic stem cells. *Stem Cells* **25**, 3143–3154.

Herlin, M., Kalantari, F., Stern, N., Sand, S., Larsson, S., Viluksela, M., Tuomisto, J. T., Tuomisto, J., Tuukkanen, J., and Jämsä, T. (2010). Quantitative characterization of changes in bone geometry, mineral density and biomechanical properties in two rat strains with different Ah-receptor structures after long-term exposure to 2,3,7,8-tetrachlorodibenzo-p-dioxin. *Toxicology* **273**, 1–11.

Jämsä, T., Viluksela, M., Tuomisto, J. T., Tuomisto, J., and Tuukkanen, J. (2001). Effects of 2,3,7,8-tetrachlorodibenzo-p-dioxin on bone in two rat strains with different aryl hydrocarbon receptor structures. *J. Bone Miner. Res.* **16**, 1812–1820.

Jensen, E. D., Gopalakrishnan, R., and Westendorf, J. J. (2010). Regulation of gene expression in osteoblasts. *Biofactors* **36**, 25–32.

Jeon, E., Yun, Y-R., Kang, W., Lee, S., Koh, Y-H., Kim, H-W., Suh, C. K., Jang, J-H. (2012) Investigating the role of FGF18 in the cultivation and osteogenic differentiation of mesenchymal stem cells. *PLoS One*, 7, e43982.

Kakutani, H., Yuzuriha, T., Akiyama, E., Nakao, T., and Ohta, S. (2018). Complex toxicity as disruption of adipocyte or osteoblast differentiation in human mesenchymal stem cells under the mixed condition of TBBPA and TCDD. *Toxicol. Rep.* **5**, 737–743.

Kawai, M., Sousa, K. M., MacDougald, O. A., and Rosen, C. J. (2010). The many facets of PPARgamma: novel insights for the skeleton. *Am. J. Physiol. Endocrinol. Metab.* **299**, E3–E9.

Klareskog, L., Padyukov, L., and Alfredsson, L. (2007). Smoking as a trigger for inflammatory rheumatic diseases. *Curr. Opin. Rheumatol.* **19**, 49–54.

Ko, C.-I., Wang, Q., Fan, Y., Xia, Y., and Puga, A. (2014). Pluripotency factors and polycomb group proteins repress aryl hydrocarbon receptor expression in murine embryonic stem cells. *Stem Cell Res.* **12**, 296–308.

Ko, C.-I., Fan, Y., de Gannes, M., Wang, Q., Xia, Y., and Puga, A. (2016). Repression of the aryl hydrocarbon receptor is required to maintain mitotic progression and prevent loss of pluripotency of embryonic stem cells. *Stem Cells* **34**, 2825–2839.

Komori, T. (2010). Regulation of bone development and extracellular matrix protein genes by RUNX2. *Cell Tissue Res.* **339**, 189–195.

Korkalainen, M., Kallio, E., Olkku, A., Nelo, K., Ilvesaro, J., Tuukkanen, J., Mahonen, A., and Viluksela, M. (2009). Dioxins interfere with differentiation of osteoblasts and osteoclasts. *Bone* **44**, 1134–1142.

Krakow, D., and Rimoin, D. L. (2010). The skeletal dysplasias. *Genet. Med.* **12**, 327–341.

Kung, M. H., Yukata, K., O'Keefe, R. J., and Zuscik, M. J. (2012). Aryl hydrocarbon receptor-mediated impairment of chondrogenesis and fracture healing by cigarette smoke and benzo(α)pyrene. *J. Cell Physiol.* **227**, 1062–1070.

Liu, P. C. C., Phillips, M. A., and Matsumura, F. (1996). Alteration by 2,3,7,8-tetrachlordibenzo-p-dioxin of CCAAT/enhancer binding protein correlates with suppression of adipocyte differentiation in 3T3-L1 cells. *Mol. Pharmacol.* **49**, 989–997.

Long, F. (2012). Building strong bones: molecular regulation of the osteoblast lineage. *Nat. Rev. Mol. Cell Biol.* **13**, 27–38.

Lu, J., Dai, J., Wang, X., Zhang, M., Zhang, P., Sun, H., Zhang, XLi., Yu, H., Zhang, WBin., Zhang, L., *et al.* (2014). The effect of fibroblast growth factor 9 on the osteogenic differentiation of Calvaria-derived mesenchymal cells. *J. Craniofac. Surg.* **25**, e502–e505.

Lu, J., Dai, J., Wang, X., Zhang, M., Zhang, P., Sun, H., Zhang, X., Yu, H., Zhang, W., Zhang, L., *et al.* (2015). Effect of fibroblast growth factor 9 on the osteogenic differentiation of bone marrow stromal stem cells and dental pulp stem cells. *Mol. Med. Rep.* **11**, 1661–1668.

Mansukhani, A., Ambrosetti, D., Holmes, G., Cornivelli, L., and Basilico, C. (2005). Sox2 induction by FGF and FGFR2 activating mutations inhibits Wnt signaling and osteoblast differentiation. *J. Cell Biol.* **168**, 1065–1076.

McCormack, S.E., Cousminer, D.L., Chesi, A., Mitchell, J.A., Roy, S.M., Kalkwarf, H.J., Lappe, J.M., Gilsanz, V., Oberfield, S.E., and Shepherd, J.A. (2017). Association between linear growth and bone accrual in a diverse cohort of children and adolescents. *JAMA Pediatr.* **19104**, 1–9.

Miettinen, H. M., Pulkkinen, P., Jämsä, T., Koistinen, J., Simanainen, U., Tuomisto, J., Tuukkanen, J., and Viluksela, M. (2005). Effects of in utero and lactational TCDD exposure on bone development in differentially sensitive rat lines. *Toxicol. Sci.* **85**, 1003–1012.

Narkowicz, S., Polkowska, Ż., Kiełbratowska, B., and Namieśnik, J. (2013). Environmental tobacco smoke: exposure, health effects, and analysis. *Crit. Rev. Environ. Sci. Tech.* **43**, 121–161.

Pillai, H. K., Fang, M., Beglov, D., Kozakov, D., Vajda, S., Stapleton, H. M., Webster, T. F., and Schlezinger, J. J. (2014). Ligand binding and activation of PPARγ by Firemaster 550: effects on adipogenesis and osteogenesis in vitro. *Environ. Health Perspect.* **122**, 1225–1232.

Podechard, N., Fardel, O., Corolleur, M., Bernard, M., and Lecureur, V. (2009). Inhibition of human mesenchymal stem cell-derived adipogenesis by the environmental contaminant benzo(a)pyrene. *Toxicol. In Vitro* **23**, 1139–1144.

Riekstina, U., Cakstina, I., Parfejevs, V., Hoogduijn, M., Jankovskis, G., Muiznieks, I., Muceniece, R., and Ancans, J. (2009). Embryonic stem cell marker expression pattern in human mesenchymal stem cells derived from bone marrow, adipose tissue, heart and dermis. *Stem Cell Rev. Rep.* **5**, 378–386.

Ryan, E. P., Holz, J. D., Mulcahey, M., Sheu, T.-J., Gasiewicz, T. A., and Puzas, J. E. (2007). Environmental toxicants may modulate osteoblast differentiation by a mechanism involving the aryl hydrocarbon receptor. *J. Bone Miner. Res.* **22**, 1571–1580.

Sakaguchi, Y., Sekiya, I., Yagishita, K., Ichinose, S., Shinomiya, K., and Muneta, T. (2004). Suspended cells from trabecular bone by collagenase digestion become virtually identical to mesenchymal stem cells obtained from marrow. *Stem Cells* **104**, 2728–2735.

Seo, E., Basu-Roy, U., Zavadil, J., Basilico, C., and Mansukhani, A. (2011). Distinct functions of Sox2 control self-renewal and differentiation in the osteoblast lineage. *Mol. Cell Biol.* **31**, 4593–4608.

Shimba, S., Wada, T., and Tezuka, M. (2001). Aryl hydrocarbon receptor (AhR) is involved in negative regulation of adipose differentiation in 3T3-L1 cells: ahR inhibits adipose differentiation independently of dioxin. *J. Cell Sci.* **114**, 2809–2817.

Singh, K. P., Wyman, A., Casado, F. L., Garrett, R. W., and Gasiewicz, T. A. (2009). Treatment of mice with the Ah receptor agonist and human carcinogen dioxin results in altered numbers and function of hematopoietic stem cells. *Carcinogenesis* **30**, 11–19.

Sinha, K. M., and Zhou, X. (2013). Genetic and molecular control of osterix in skeletal formation. *J. Cell. Biochem.* **114**, 975–984.

Smith, K. J., Murray, I., Tanos, R., Tellew, J., Boitano, A. E., Bisson, W. H., Kolluri, S. K., Cooke, M. P., and Perdew, G. H. (2011). Identification of a high-affinity ligand that exhibits complete aryl hydrocarbon receptor antagonism. *J. Pharmacol. Exp. Ther.* **338**, 318–327.

Spandidos, A., Wang, X., Wang, H., and Seed, B. (2010). PrimerBank: a resource of human and mouse PCR primer pairs for gene expression detection and quantification. *Nucleic Acids Res.* **38**, D792–D799.

Su, N., Du, X., and Chen, L. (2008). FGF signaling: its role in bone development and human skeletal diseases. *Front. Biosci.* **13**, 2842–2865.

Ueng, T. H., Hung, C.-C., Kuo, M.-L., Chan, P.-K., Hu, S.-H., Yang, P.-C., and Chang, L. W. (2005). Induction of fibroblast growth factor-9 and interleukin-1α gene expression by motorcycle exhaust particulate extracts and benzo(a)pyrene in human lung adenocarcinoma cells. *Toxicol. Sci.* **87**, 483–496.

Wang, C.-K., Chang, H., Chen, P.-H., Chang, J. T., Kuo, Y.-C., Ko, J.-L., and Lin, P. (2009). Aryl hydrocarbon receptor activation and overexpression upregulated fibroblast growth factor-9 in human lung adenocarcinomas. *Int. J. Cancer* **125**, 807–815.

Wang, Y., Fan, Y., and Puga, A. (2010). Dioxin exposure disrupts the differentiation of mouse embryonic stem cells into cardiomyocytes. *Toxicol. Sci.* **115**, 225–237.

Wang, Z., Oron, E., Nelson, B., Razis, S., and Ivanova, N. (2012). Distinct lineage specification roles for NANOG, OCT4, and SOX2 in human embryonic stem cells. *Cell Stem Cell* **10**, 440–454.

Ward, K. D., and Klesges, R. C. (2001). A meta-analysis of the effects of cigarette smoking on bone mineral density. *Calcif. Tissue Int.* **68**, 259–270.

Watson, A. T. D., Planchart, A., Mattingly, C. J., Winkler, C., Reif, D. M., and Kullman, S. W. (2017). Embryonic exposure to TCDD impacts osteogenesis of the axial skeleton in Japanese medaka, Oryzias latipes. *Toxicol. Sci.* **155**, 485–496.

Watt, J., and Schlezinger, J. J. (2015). Structurally-diverse, PPARγ-activating environmental toxicants induce adipogenesis and suppress osteogenesis in bone marrow mesenchymal stromal cells. *Toxicology* **331**, 66–77.

Yu, T.-Y., Kondo, T., Matsumoto, T., Fujii-Kuriyama, Y., and Imai, Y. (2014). Aryl hydrocarbon receptor catabolic activity in bone metabolism is osteoclast dependent in vivo. *Biochem. Biophys. Res. Commun.* **450**, 416–422.